Received 30 January 2024; revised 4 April 2024; accepted 8 April 2024. Date of publication 10 April 2024; date of current version 24 April 2024.
The review of this article was arranged by Editor Z. Zhang.

Digital Object Identifier 10.1109/JEDS.2024.3387324

Tungsten Trioxide Nanoparticles Modified Cuprous Oxide Film Non-Enzymatic Dopamine Sensor

JUNG-CHUAN CHOU [1] (Senior Member, IEEE), WEI-SHUN CHEN [1], PO-HUI YANG [1] (Member, IEEE), PO-YU KUO [1] (Member, IEEE), CHIH-HSIEN LAI [1] (Member, IEEE), AND YU-HSUN NIEN [2] (Member, IEEE)

1 Graduate School of Electronic Engineering, National Yunlin University of Science and Technology, Douliu 64002, Taiwan
2 Graduate School of Chemical and Materials Engineering, National Yunlin University of Science and Technology, Douliu 64002, Taiwan

CORRESPONDING AUTHOR: J.-C. CHOU (e-mail: choujc@yuntech.edu.tw)

This work was supported by the National Science and Technology Council, Taiwan, Republic of China, under Grant NSTC 111-2221-E-224-058 and Grant NSTC 112-2221-E-224-049.

ABSTRACT Non-enzymatic dopamine (DA) sensors are important in diagnosing and treating human diseases. However, non-enzymatic sensors frequently encounter interference from other substances, posing a challenge of poor selectivity for such sensors. Herein, we prepared tungsten trioxide nanoparticles (WO_3 NPs) via a simple hydrothermal method and immobilized them onto a cuprous oxide (Cu_2O) film. The results demonstrate that WO_3 NPs offer improved selectivity, thus avoiding interference from other substances. The DA sensor based on the Cu_2O film modified with WO_3 NPs exhibits excellent DA detection performance, with a wide linear range of 1 μM to 10 mM, a low limit of detection of 0.21 μM, and good selectivity against common interfering substances. This non-enzymatic DA sensor features a simple structure, easy fabrication, small size, and suitability for mass production.

INDEX TERMS Cuprous oxide (Cu_2O), tungsten trioxide nanoparticles (WO_3 NPs), dopamine (DA) sensor.

I. INTRODUCTION

Dopamine (DA), categorized as one of the catecholamines, is a neurotransmitter originating in the brain, facilitating intercellular communication through chemical signaling [1]. A DA deficiency is linked to psychiatric conditions like parkinsonism and attention deficit hyperactivity disorder (ADHD) [2]. Consequently, the detection of DA holds significant importance. Over recent years, numerous electrochemical biosensors have emerged to detect DA [3]. Tyrosinase-based DA sensors have attracted extensive attention among researchers [4]. However, the temperature factor can easily affect tyrosinase, making it difficult to preserve [5]. Therefore, research into non-enzymatic DA sensors has emerged as a new direction.

For non-enzymatic sensors, their applications can improve several inherent problems associated with enzymatic sensors, including price, poor stability, and influence on temperature. Therefore, this study mainly analyzes non-enzymatic sensors. Non-enzymatic sensors are primarily based on metal oxides [6], precious metals [7], conductive polymers [8], and carbonaceous materials [9] as sensing materials. Among them, metal oxides have several important advantages for sensors, including the easy formation of various nanostructures [10], excellent electrical conductivity, and low cost [11].

Based on the advantages of metal oxides, in this study, we employed cuprous oxide (Cu_2O) and tungsten trioxide (WO_3) as sensing materials for DA detection. Cu_2O was chosen as the sensing layer due to its impressive electrocatalytic performance, strong biocompatibility, and expansive specific surface area, which can enhance DA sensing [12]. However, despite these advantages, Cu_2O is sensitive to various biomolecules, leading to the detection of interfering substances such as fructose, glucose, and urea during the measurement process. To address this issue, we utilized WO_3, which exhibits specificity to DA, to modify Cu_2O and enhance selectivity [13]. In addition to

its specificity to DA, WO_3 offers low cost and excellent electrical conductivity [14]. These beneficial properties help reduce temperature effects and improve the reliability of DA measurement.

Many detection techniques exist for DA, such as fluorescence [15] and spectrophotometry [16]. Fluorescence spectrophotometry are the suitable choices for luminescent or quantum-sized materials, which fluorescence spectrometers can analyze. However, the most significant difficulties are the high threshold of operation technology. Spectrophotometry relies on the ability of materials to absorb visible light to ascertain DA concentration based on absorbance. However, this method has a relatively low accurate rate, a significant drawback. As a result, among the plethora of DA detection techniques available, electrochemical techniques are widely regarded as the most suitable measurement methods for human environments. Standard electrochemical analyses include cyclic voltammetry, differential pulse voltammetry, and square wave voltammetry [17], [18], [19]. However, current-based techniques may lead to sensing film detachment, compromising stability [20]. Potentiometric measurement technology was employed in this study to characterize the sensor and addressed this issue. Unlike current-based methods, potentiometry utilizes low-bias currents, minimizing the risk of sensing film detachment and enhancing sensor stability [20]. In addition, potentiometric measurement technology has a small size and highly stable characteristics. Many different potentiometric sensors have been developed so far [21].

II. EXPERIMENTAL

A. MATERIALS

The DA sensor utilizes polyethylene terephthalate (PET) as its substrate. We prepare the sensor conductive wires and electrodes from silver paste, while epoxy constitutes the protective layer. Sputtering with a CuO target forms the Cu_2O film. Tungsten hexachloride and urea powder serve as the precursor for WO_3 NPs. We mix DA hydrochloride powder with phosphate-buffered saline (PBS) solution to prepare the DA solution. We incorporate interferents such as ascorbic acid powder, uric acid powder, urea powder, fructose powder, and glucose powder in the interference effects.

B. PREPARATION OF THE CUPROUS OXIDE (CU_2O) FILM

The sputtering technique is renowned for its reliability in producing high-quality film, primarily attributed to the flat and uniform surface characteristic of films prepared using the radio frequency (RF) sputtering system [22]. We utilized a CuO target as the deposition material in our sensor fabrication process. During sputtering, the ratio of oxygen to argon plays a crucial role as it directly influences the formation of the Cu_2O film. Therefore, we introduced a specific oxygen-to-argon ratio set at 5:13 in our ratio. This ratio is selected because lower oxidizing conditions favor the existence of copper ions in the +1 valence state, corresponding to the chemical state of Cu_2O. Conversely, in a high-oxygen environment, copper ions are more likely to exist in the +2 valence state, forming CuO. Furthermore, we maintained a deposition pressure of 10 mTorr, applied power of 40 W, and conducted the deposition process for 30 minutes. These parameters are meticulously chosen to ensure optimal film quality and sensor performance.

C. PREPARATION OF THE TUNGSTEN TRIOXIDE NANOPARTICLES (WO_3 NPS)

The hydrothermal method for synthesizing WO_3 NPs offers a cost-effective and straightforward approach. In our procedure, we used tungsten hexachloride and urea as precursors dissolved in 40 ml of 99.5% ethanol. Initially, the tungsten hexachloride, urea, and ethanol were thoroughly mixed and stirred for 3 hours. Subsequently, the solution was transferred into a Teflon lining and placed inside an autoclave, maintaining a temperature of 180 °C for 12 hours. Following hydrothermal treatment, the resulting precipitate was collected and washed with 99.5% ethanol to eliminate impurities. The residue was then dried in an oven at 60 °C for 24 hours, yielding a yellow powder. Finally, the obtained powder underwent annealing at 450 °C for 3 hours, facilitating the formation of pristine WO_3 NPs [23]. This synthesis route ensures the production of high-quality WO_3 NPs.

D. PREPARATION OF THE WO_3 NPS/CU_2O/SILVER/PET DOPAMINE SENSOR

To clean the PET substrate, we sequentially immersed it in acetone, alcohol, and deionized water and cleaned it with an ultrasonic cleaner. Next, a nitrogen gun was used to remove the excess water from the PET substrate. Finally, a screen printing machine printed the silver paste on the PET substrate as a conductive wire. Figure 1(a) is the appearance of the sensor. The sensor is 4 cm × 3 cm and has one reference electrode, a counter electrode, and six working electrodes. Each working electrode has an area of 0.138 cm^2. After preparing the wires, the CuO target and RF sputtering system deposit Cu_2O film on the working electrode. Then, the screen printing machine will print epoxy resin on the outside of the sensor as a protective layer. We extracted a 2 μL solution of WO_3 NPs, and through the drop-casting method, we modified it onto the Cu_2O film, heating it to 70 °C for enhanced adherence. Volumes less than 2 μL cannot completely cover the working electrode surface, while volumes greater than 2 μL lead to overflowing the WO_3 NPs solution from the working electrode surface. For these reasons, we chose a 2 μL WO_3 NPs solution for modification. Figure 1(b) is the structure of the sensor. After the above steps, the structure of the DA sensor is WO_3 NPs/Cu_2O/Silver/PET.

E. SENSOR MEASUREMENT SYSTEM

All analyses and measurements in this study were carried out using a voltage-time (V-T) measurement system. The

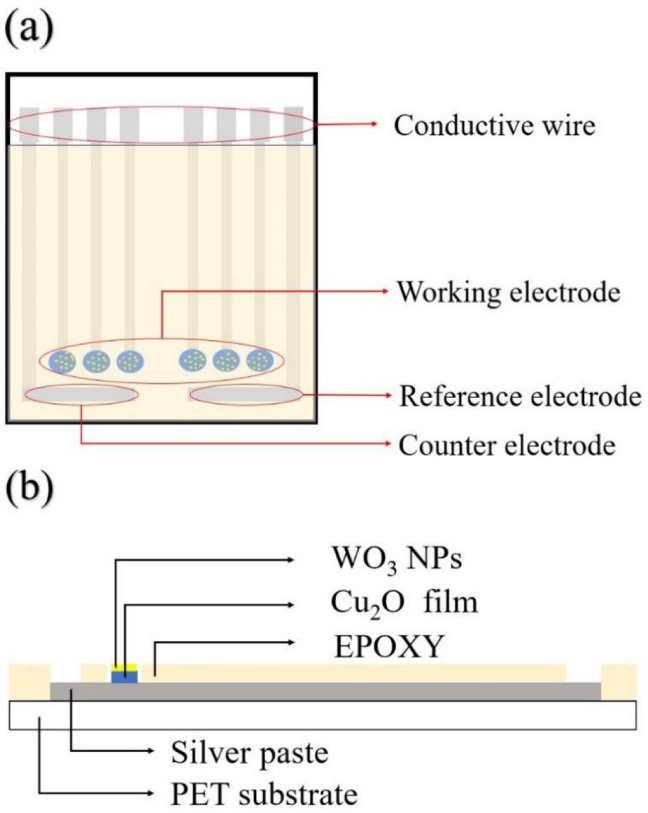

FIGURE 1. (a) Top view of the dopamine sensor, and (b) a side view illustrating the structure of the dopamine sensor.

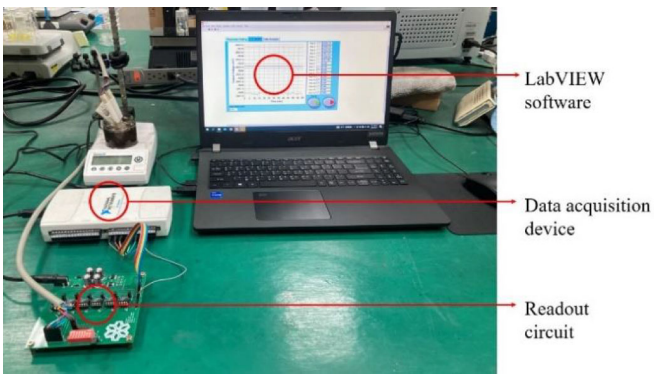

FIGURE 2. V-T measurement system.

V-T measurement system comprises several components, including LabVIEW software, DA sensor and DA solution, readout circuit, and data acquisition device. Figure 2 depicts the components of the V-T measurement system. This system works by briefly immersing the DA sensor in a DA solution. Interaction between the working electrode of the sensor and the DA solution produces a change in the response voltage, where the module of the readout circuit is LT1167. Then, the data acquisition device converts the analog signal into a digital signal suitable for computer processing. Finally, the LabVIEW software facilitates the display of the signal on a computer screen and performs further analysis of the voltage-time data. The V-T measurement system provides an excellent framework for accurate, flexible, and simplified sensor analysis. The LT1167 used in the readout circuit provides high input impedance and common-mode rejection ratio to ensure accurate measurement of response voltage; low power supply noise minimizes interference, thereby achieving accurate and reliable measurements, and LabVIEW software allows customized data visualization, analysis, and control to meet various experimental requirements [24]. In summary, the V-T measurement system, with its carefully selected components and robust operating principle, provides accurate, precise, and efficient measurement capabilities for analyzing the response over time of the sensor.

III. RESULT AND DISCUSSION

A. REACTION MECHANISM BETWEEN THE WO_3 NPS AND THE DOPAMINE

In this study, we propose a DA sensor in which WO_3 is used to modify the working electrode to enhance sensitivity and selectivity. The reaction of WO_3 NPs with DA is shown in formula (1) [25], leading to DA oxidation to dopamine-o-quinone (DAQ). This process produces two hydrogen ions (H^+) and two electrons (e^-). The formed electrons are the product of the oxidation process, which can be measured. Thus, the measured electrons enable us to determine the DA concentration indirectly. According to the reaction mechanism of formula (1), we can use the Nernst equation to represent it, as shown in formula (2) [26]:

$$\text{Dopamine (DA)} \xrightarrow{WO_3NPs} \text{dopamine-o-quinone (DAQ)} + 2H^+ + 2e^- \tag{1}$$

$$E = E^0 + \frac{0.059}{2} \times \log \frac{[DAQ][H^+]^2}{[DA]} \tag{2}$$

E in formula (2) represents the response voltage of the DA sensor, and E^0 represents the initial potential.

B. SEM AND EDS ANALYSIS OF THE CU_2O FILM AND THE WO_3 NPS

We performed the surface analysis of Cu_2O film and WO_3 NPs using field emission scanning electron microscopy (FE-SEM). The instrument models used were JSM-7610FPlus and JSM-6701F, which are made in Japan. Figure 3(a) depicts a cross-sectional photo of the Cu_2O film. The thickness of the Cu_2O film we prepared is about 329 nm. Additionally, as shown in Fig. 3(b), the Cu_2O film contains closely arranged particles with an average particle size of 33.69 nm. Thus, this proved the compactness of the Cu_2O film. Figure 3(c) exhibits the top view photo of WO_3 NPs, and the average particle size of WO_3 NPs is 66.89 nm. We also analyzed the Cu_2O film and WO_3 NPs using energy-dispersive X-ray (EDX) imaging. From Fig. 4 (a), it can be observed that the distribution of Cu and O elements is uniform. By analyzing the WO_3 NPs using EDX imaging, an uniform distribution of W and O elements can be observed

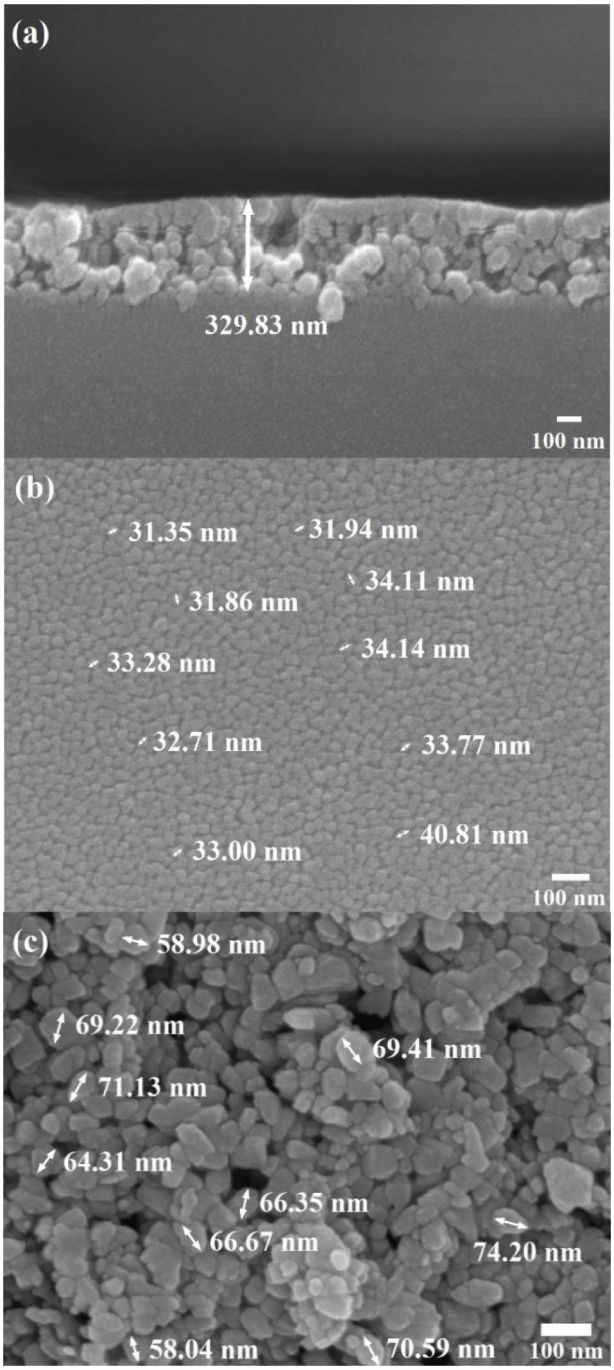

FIGURE 3. FE-SEM (a) cross-section and (b) top view images analysis of the Cu_2O film photo and (c) top view images analysis of the WO_3 NPs photo.

in Fig. 4 (b). These analyses provide valuable insights into the morphology and structure of the Cu_2O film and WO_3 NPs, which are essential for understanding their properties and performance in the sensor system.

C. XPS ANALYSIS OF THE CU_2O FILM AND THE WO_3 NPS

To verify the chemical composition of the Cu_2O film and WO_3 NPs on the working electrode, we analyzed the Cu_2O film and the WO_3 NPs by X-ray electron spectroscopy (XPS). The XPS instrument used in this study is the PHI 5000 VersaProbe III, made in Japan. Figure 5 (a) shows the O1s spectrum of the Cu_2O film. Two peaks were detected in our sub-peak fit analysis at 528.8 eV and 530.1 eV, which correspond to the binding energy between copper and oxygen and the presence of a hydroxyl group, respectively [27]. Figure 5 (b) shows the energy spectrum of Cu2p. The Cu2p spectrum displays characteristic peaks for $2p_{3/2}$ and $2p_{1/2}$, and after peak fitting, two individual peaks are shown for $2p_{3/2}$ and $2p_{1/2}$, which are attributed to Cu^+ and Cu^{2+}, respectively. The binding energies of Cu^+ are located at 931.6 eV and 951.4 eV, indicating the presence of Cu_2O in the film [28], [29], while the binding energies of Cu^{2+} are located at 933.5 eV and 953.4 eV, indicating the presence of CuO in the film [30]. The remaining three peaks at 940.1 eV, 942.6 eV, and 961.1 eV represent satellite peaks. After XPS analysis, we can find that the bonding peak of Cu^+ is larger than that of Cu^{2+}, which means that the film on the working electrode mainly comprises Cu_2O.

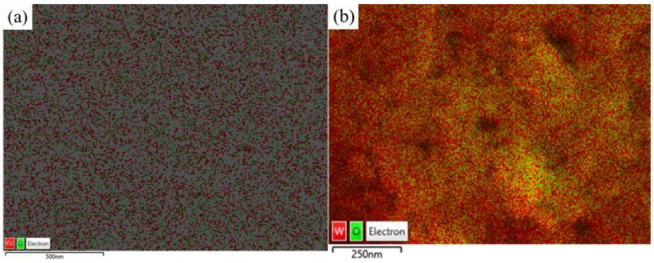

FIGURE 4. EDX mapping patterns of the (a) Cu_2O film and (b) WO_3 NPs.

Figure 5 (c) shows the O1s spectrum of the WO_3 NPs, and Figure 5 (d) shows the W4f spectrum. Two peaks are observed by fitting the O1s peak, as shown in Fig. 5 (c). The main peak at 530.5 eV corresponds to the bonding between tungsten and oxygen ions [31], while another peak at 531.5 eV corresponds to oxygen in hydroxyl groups [32]. Additionally, in Fig. 5 (d), two major XPS peaks are attributed to the characteristic doublet of W^{6+} [33]. Two peaks can be observed at 35.8 eV and 38.0 eV, representing the binding energies of W $4f_{7/2}$ and W $4f_{5/2}$, respectively. Through peak fitting, the areas of these two peaks, W $4f_{7/2}$ and W $4f_{5/2}$, as well as the two peaks in O1s, can be determined. The atomic ratio of W4f, calculated by dividing the peak area by the sensitivity factor of 3.863, is approximately 25.52 at%, and the atomic ratio of O1s is approximately 74.47 at%. These confirm a ratio of about 2.91 between O1s and W4f, which is close to 3.

D. XRD ANALYSIS OF THE CU_2O FILM AND THE WO_3 NPS

This study conducts X-ray diffraction (XRD) analysis to identify the crystalline phases of Cu_2O film and WO_3 NPs. The XRD results for the Cu_2O film, depicted in Fig. 6 (a), reveal the absence of prominent characteristic diffraction peaks, suggesting that the film is in an amorphous phase.

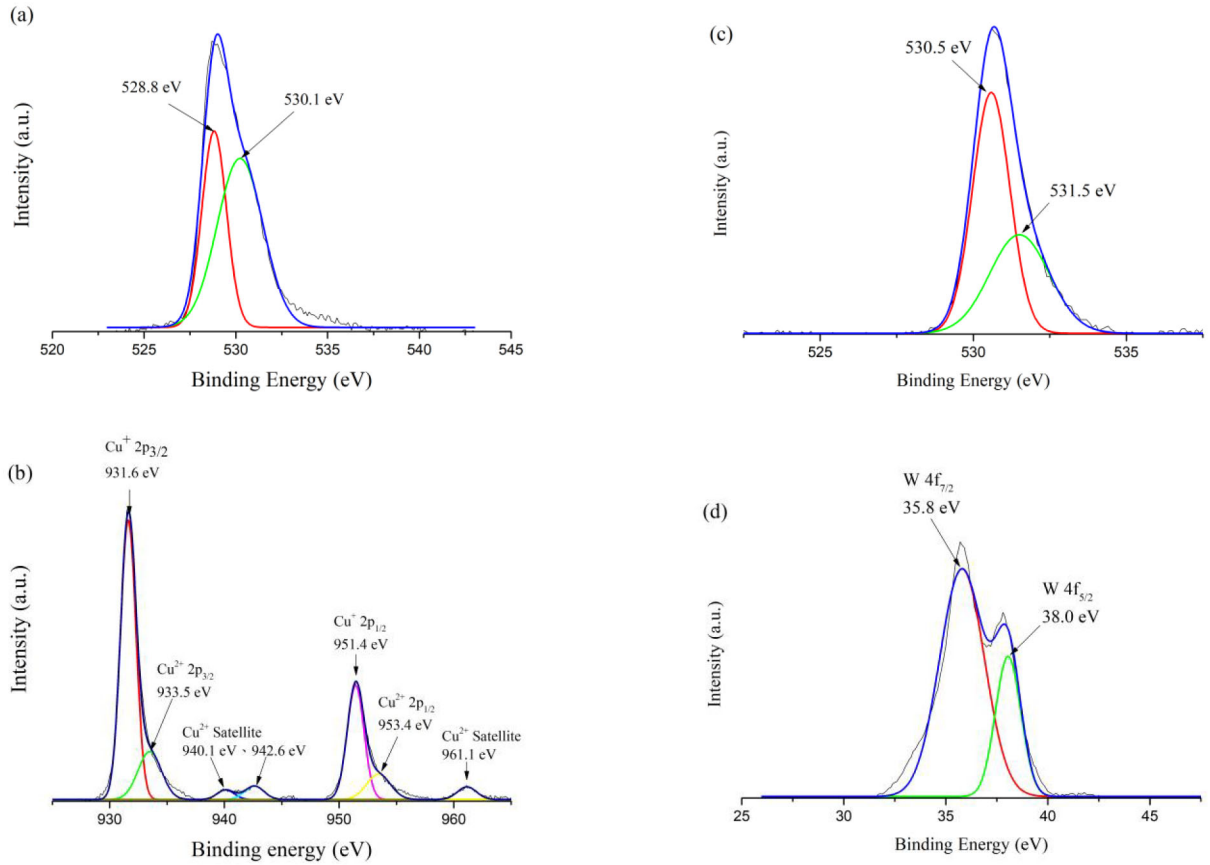

FIGURE 5. XPS spectrum of the Cu_2O film and WO_3 NPs, the XPS spectra for (a) O 1 s of the Cu_2O film, (b) Cu 2p, (c) O 1 s of the WO_3 NPs, and (d) W 4f.

Subsequently, we examined the characteristic diffraction peaks of WO_3 NPs within the range of 15° to 65°. As illustrated in Fig. 6 (b), distinct diffraction peaks are observed at specific angles, including 23.38°, 23.86°, 24.62°, 26.86°, 28.98°, 33.56°, 34.44°, 42.04°, 50.20°, and 56.18°. Comparisons of these peaks with the analysis results of the JCPDS 20-1324 standard card reveals their correspondence to the (001), (020), (200), (120), (111), (021), (220), (221), (140), and (141) planes, respectively. This correspondence confirms that the WO_3 NPs exhibit an orthorhombic crystal structure [33].

E. AVERAGE SENSITIVITY AND LINEARITY OF THE DOPAMINE SENSOR

Our measurement range spans from 1μM to 10 mM, based on the typical concentrations of DA found in human urine [34], [35], [36]. The average sensitivity of a sensor is a crucial indicator of its responsiveness to varying concentrations of DA. It quantifies the magnitude of the voltage change observed in response to different concentrations of DA. Linearity is a crucial parameter that assesses the accuracy of a sensor for measuring various concentrations of DA. A linear value closer to one indicates a higher degree of accuracy exhibited by the sensor. Essentially, a sensor with excellent linearity maintains a consistent relationship between the measured response and the corresponding concentration of DA across a wide range of concentrations. Figure 7 (a) and (b) illustrates the average sensitivity and linearity of two types of sensors. The average sensitivity of the Cu_2O/Silver/PET DA sensor is 12.82 mV/decade, with a corresponding linearity of 0.995.

In contrast, the WO_3 NPs/Cu_2O/Silver/PET DA sensor exhibits a higher average sensitivity of 26.60 mV/decade, with a corresponding linearity of 0.992. According to the experimental findings, the catalytic performance of the Cu_2O DA sensor, enhanced with WO_3 NPs, demonstrates a significant improvement compared to the pure Cu_2O DA sensor. This enhancement is evidenced by an over two-fold increase in the average sensitivity of the sensor.

F. INTERFERENCE EFFECTS OF THE DOPAMINE SENSOR

The selectivity of a sensor refers to its ability to distinguish and accurately measure the target analyze in the presence of interferents [37]. In the case of DA sensors, interferents in urine or blood can lead to false positive or false negative results [38]. Thus, it is crucial to evaluate the selectivity of the sensor. In this experiment, the sensor selectivity was evaluated by adding interferents commonly found in urine or blood to the sensor and measuring their effect on the response voltage. The interferents used were fructose (Fru), glucose (Glu), urea (UR), uric acid (UA), and ascorbic acid (AA), in addition to DA. The concentrations of various

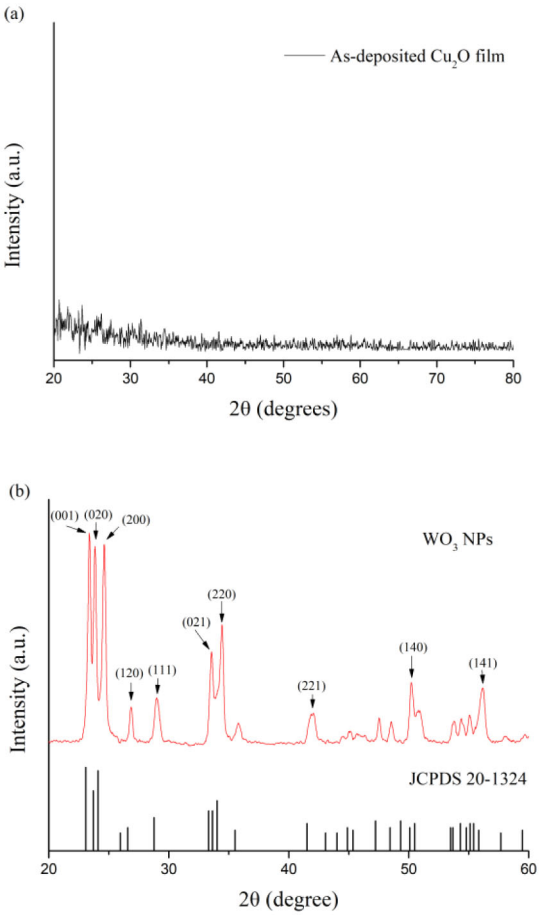

FIGURE 6. XRD patterns of the (a) Cu_2O film and (b) WO_3 NPs.

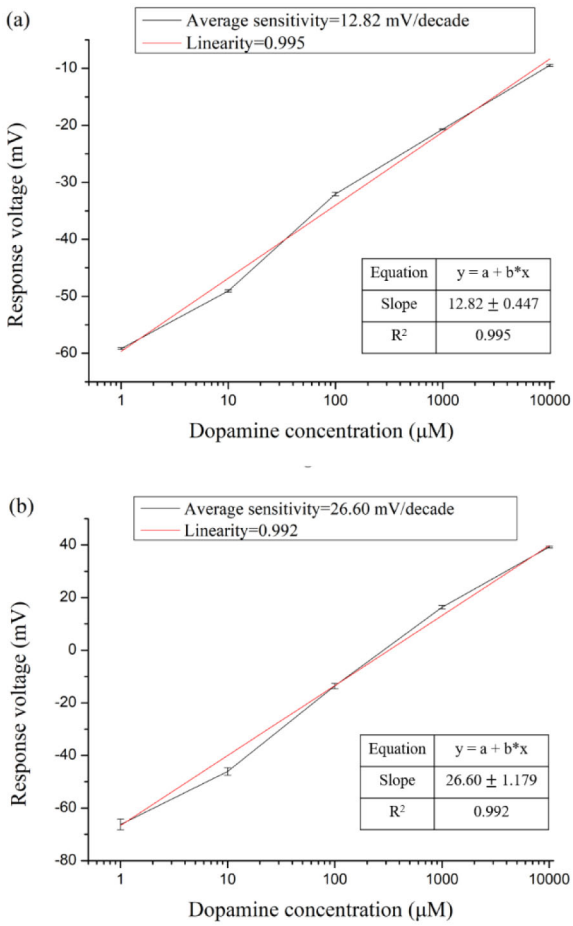

FIGURE 7. Average sensitivity and linearity of (a) the Cu_2O/Silver/PET, (b) the WO_3 NPs/Cu_2O/Silver/PET dopamine sensor.

interfering substances were chosen within the normal range of human [39], [40], [41], [42], [43]. Figure 8 shows sensors with two different structures. The results showed that the interferents easily affected the Cu_2O/Silver/PET DA sensor and did not exhibit significant selectivity for DA. 0Conversely, the WO_3 NPs/Cu_2O/Silver/PET DA sensor exhibited enhanced selectivity for DA, effectively mitigating the impact of other interferents. This improvement can be attributed to WO_3 NPs, which promote the chemical reaction between DA and the sensor while concurrently minimizing reactions with interferents [44]. The experimental results of this study indicate that the WO_3 NPs/Cu_2O/Silver/PET DA sensor demonstrates superior selectivity compared to the Cu_2O/Silver/PET DA sensor.

G. LOD OF THE DOPAMINE SENSOR

The limit of detection (LOD) is a pivotal parameter in sensor performance assessment, as it signifies the minimum concentration of biomolecules detectable with accuracy. For instance, urine DA concentrations typically fluctuate between 0.3 μM to 2.5 μM over a day [45]. Consequently, the LOD of the sensor must be lower than this range to ensure effective detection. In this experiment, two DA sensors with distinct structures were employed for measurement. The experimental procedure is as follows: first, the sensor was immersed in pure PBS solution without DA to measure its response voltage and use it as the initial concentration (C_{base}). Then, the sensor was immersed in DA solutions ranging from 1 μM to 10 mM to measure the average sensing degree (S_0). To calculate the standard deviation (σ) of the response voltage, we utilized formula (3) [46], where X represents the response voltage in pure phosphate-buffered saline (PBS) solution, "$\overline{X}$" denotes the average value of the response voltage, and n signifies the number of sensor samples. Subsequently, the obtained standard deviation (σ), along with the average sensing degree (S_0) and the initial concentration (C_{base}), were utilized in formula (4) [47]. The calculation established the LOD for the Cu_2O/Silver/PET DA sensor at 0.75 μM. Meanwhile, it figured out the LOD for the WO_3 NPs/Cu_2O/Silver/PET DA sensor to be 0.21 μM. The experimental results show that the LOD of the sensor can be reduced by modifying the WO_3 NPs, which enables the sensor to measure the minimum value of DA concentration in urine. The LOD of 0.21 μM achieved by the WO_3 NPs/Cu_2O/Silver/PET DA sensor is lower than the reported DA concentration in human urine, indicating that this sensor can be potentially applied for detecting DA in

TABLE 1. Performance between different structures of the dopamine sensors.

Sensor structure	Average sensitivity (mV/decade)	LOD (μM)	Concentration range	References
Cu_2O/Silver/PET	12.82	0.75	1 μM - 10 mM	This work
WO_3 NPs/ Cu_2O/Silver/PET	26.60	0.21	1 μM - 10 mM	This work
PBPA/KTFPB/PVC/DOS	56.0	0.8	0.03 μM - 10 mM	[34] 2019
PBBB/KTFPB/PVC/DOS	56.5	0.8	0.03 μM - 10 mM	[34] 2019
PSS/PEDOT/PVC	53.85	5.8	0.1 μM - 100 mM	[35] 2021
DOP-IP/PVC	60.28	0.37	1 μM - 100 mM	[36] 2022
Laccase/OFET	N/A	0.19	1 μM - 0.5 mM	[50] 2023
Nafion/Tyrosinase/ RuO_2/ENIG	77.58	0.12	1 μM - 10 mM	[51] 2024

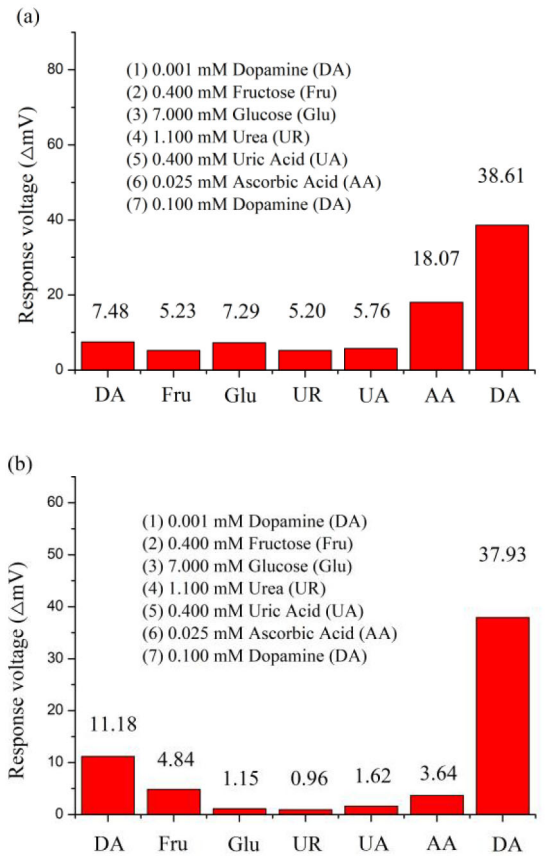

FIGURE 8. Interference effects of (a) the Cu_2O/Silver/PET, (b) the WO_3 NPs/Cu_2O/Silver/PET dopamine sensor.

clinical samples.

$$\sigma = \sqrt{\frac{\sum |X - \overline{X}|^2}{n - 1}} \tag{3}$$

$$C_{LOD} = \frac{3\sigma}{S_0} + C_{base} \tag{4}$$

H. REPRODUCIBILITY OF THE DOPAMINE SENSOR

Reproducibility experiments were conducted to determine the accuracy and precision of the DA sensors [48]. Six identical sensors were prepared and immersed in DA solutions of varying concentrations, including 10 mM, 1 mM, 100 μM, 10 μM, and 1 μM. The average sensitivity and linearity of the six sensors were calculated after measurements. The measurement results of two sets of six sensors with different structures are presented in Fig. 9. Subsequently, the relative standard deviation (RSD) was calculated for the measurements. The RSD of the Cu_2O/Silver/PET DA sensor is 2.8%, while that of the WO_3 NPs/Cu_2O/Silver/PET DA sensor is 4.2%. While the RSD of the WO_3 NPs/Cu_2O/Silver/PET DA sensor is higher compared to the Cu_2O/Silver/PET DA sensor, we can observe that all six sets of DA sensors have improved the overall average sensitivity level with the modification of WO_3 NPs. Additionally, the RSD value of the WO_3 NPs/Cu_2O/Silver/PET DA sensor is less than 5%, which is an acceptable range for sensors [49].

I. PERFORMANCE BETWEEN DIFFERENT STRUCTURES OF THE DOPAMINE SENSORS

This study compared DA sensors with different structures regarding average sensitivity and LOD. Table 1 shows related research on DA sensors in recent years. Durka et al. [34] two pyrimidine compounds with either two phenylboronic acid groups or two phenyloxoboronic acid groups (PBPA and PBBB) were developed as polymer films for DA receptors in ion-selective electrodes (PVC/DOS). The addition of tetra (trifluoromethylphenyl) borate potassium (KTFPB) can improve the response sensitivity and detection limit of the sensor. The structure of the sensor was PBPA/KTFPB/PVC/DOS and PBBB/KTFPB/PVC/DOS. He et al. [35] a conductive polymer, poly (3,4-ethylenedioxythiophene) (PEDOT) doped with polystyrene sulfonate (PSS), was studied as a DA - selective membrane for a sensor, with polyvinyl chloride (PVC) as the membrane matrix, and the structure was PSS/PEDOT/PVC. Dere et al. [36] developed a novel solid-state polyvinyl chloride (PVC) film DA sensor. The film is composed of MIP, bis (2-ethylhexyl) sebacate (DOS), PVC, and potassiumtetrakis (4-chlorophenyl) borate (KTpClPB), and the sensor structure is DOP-IP/PVC. Ohshiro et al. [50] developed a DA sensor based on an extended-gate-type organic field-effect transistor (OFET). Laccase is the main

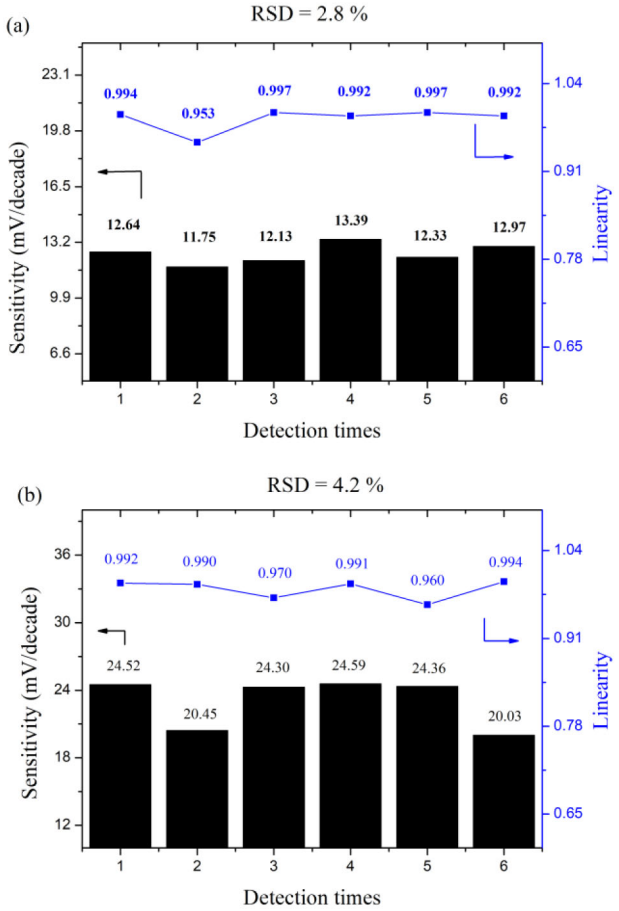

FIGURE 9. **Reproducibility of (a) the Cu_2O/Silver/PET, (b) the WO_3 NPs/Cu_2O/Silver/PET dopamine sensor.**

material for sensing DA, and its structure is Laccase/OFET. Kuo et al. [51] prepared a DA sensor based on flexible printed circuit boards (FPCBs), using RuO_2 as the sensing layer and adding tyrosinase and Nafion to detect DA. The structure is Nafion/Tyrosinase/RuO_2/FPCBs. According to the results shown in Table 1, although the average sensitivity of our prepared DA sensor does not exceed that of other DA sensors, our LOD is lower than the concentration of DA in human urine (0.3 μM to 2.5 μM). It is easier to manage because it does not require preserving delicate enzymes. Moreover, it has demonstrated the ability to detect DA within the range of 1 μM to 10 mM, and its good anti-interference ability can avoid interference from other biomolecules.

IV. CONCLUSION

In this study, we successfully developed a DA sensor utilizing WO_3 NPs with a Cu_2O film. The incorporation of WO_3 NPs resulted in a notable enhancement in sensor performance. Specifically, the average sensitivity increased from 12.82 mV/decade to 26.60 mV/decade, while the LOD improved from 0.75 μM to 0.21 μM, owing to the heightened catalytic activity of WO_3 NPs towards DA. Moreover, interference testing demonstrated a substantial enhancement in the anti-interference capability of the sensor. The reproducibility of the sensor was also excellent, indicative of a stable preparation process. Overall, this sensor is considered beneficial to the applications of non-enzyme DA sensors in the biomedical industry.

REFERENCES

[1] A. F. Arnsten, "Catecholamine regulation of the prefrontal cortex," *J. Psychopharmacol.*, vol. 11, no. 2, pp. 151–162, Mar. 1997.
[2] S. D. Iversen, and L. L. Iversen, "Dopamine: 50 years in perspective," *Trends Neurosci.*, vol. 30, no. 5, pp. 188–193, May 2007.
[3] A. Omar, A. M. Bayoumy, and A. A. Aly, "Functionalized graphene oxide with chitosan for dopamine biosensing," *J. Funct. Biomater.*, vol. 13, p. 48, Apr. 2022.
[4] C. Y. Liu, Y. C. Chou, J. H. Tsai, T. M. Huang, J. Z. Chen, and Y. C. Yeh, "Tyrosinase/chitosan/reduced graphene oxide modified screen-printed carbon electrode for sensitive and interference-free detection of dopamine," *Appl. Sci.*, vol. 9, p. 622, Feb. 2019.
[5] Z. Tang, K. Jiang, S. Sun, S. Qian, Y. Wang, and H. Lin, "A conjugated carbon-dot-tyrosinase bioprobe for highly selective and sensitive detection of dopamine," *Analyst*, vol. 144, no. 2, pp. 468–473, Oct. 2018.
[6] E. Fazio et al., "Metal-oxide based nanomaterials: Synthesis, characterization and their applications in electrical and electrochemical sensors," *Sensors*, vol. 21, p. 2494, Apr. 2021.
[7] X. Hui, X. Xuan, J. Kim, and J. Y. Park, "A highly flexible and selective dopamine sensor based on pt-au nanoparticle-modified laser-induced graphene," *Electrochimica Acta*, vol. 328, Dec. 2019, Art. no. 135066.
[8] J. S. Lee, J. Oh, S. G. Kim, and J. Jang, "Highly sensitive and selective field-effect-transistor nonenzyme dopamine sensors based on Pt/conducting polymer hybrid nanoparticles," *Small*, vol. 11, no. 20, pp. 2399–2406, Jan. 2015.
[9] S. Islam, S. Shaheen Shah, S. Naher, M. Ali Ehsan, M. A. Aziz, and A. S. Ahammad, "Graphene and carbon nanotube-based electrochemical sensing platforms for dopamine," *Chem. Asian J.*, vol. 16, no. 22, pp. 3516–3543, Sep. 2021.
[10] T. Guo, M. S. Yao, Y. H. Lin, and C. W. Nan, "A comprehensive review on synthesis methods for transition-metal oxide nanostructures," *CrystEngComm*, vol. 17, no. 19, pp. 3551–3585, Feb. 2015.
[11] P. R. Solanki, A. Kaushik, V. V. Agrawal, and B. D. Malhotra, "Nanostructured metal oxide-based biosensors," *NPG Asia Mater.*, vol. 3, no. 1, pp. 17–24, Jan. 2011.
[12] S. Sun, X. Zhang, Q. Yang, S. Liang, X. Zhang, and Z. Yang, "Cuprous oxide (Cu_2O) crystals with tailored architectures: A comprehensive review on synthesis, fundamental properties, functional modifications and applications," *Progress Mater. Sci.*, vol. 96, pp. 111–173, Jul. 2018.
[13] A. Anithaa, N. Lavanya, K. Asokan, and C. Sekar, "WO_3 Nanoparticles based direct electrochemical dopamine sensor in the presence of ascorbic acid," *Electrochimica Acta*, vol. 167, pp. 294–302, Jun. 2015.
[14] Y. Yao, D. Sang, L. Zou, Q. Wang, and C. Liu, "A review on the properties and applications of WO_3 nanostructure-based optical and electronic devices," *Nanomaterials*, vol. 11, pp. 1–24, Aug. 2021.
[15] A. Yildirim and M. Bayindir, "Turn-on fluorescent dopamine sensing based on in situ formation of visible light emitting polydopamine nanoparticles," *Anal. Chem.*, vol. 86, no. 11, pp. 5508–5512, May 2014.
[16] L. Li et al., "Ultra-sensitive surface enhanced raman spectroscopy sensor for in-situ monitoring of dopamine release using zipper-like ortho-nanodimers," *Biosensors Bioelectron.*, vol. 180, May 2021, Art. no. 113100.
[17] J. E. Koehne et al., "Carbon nanofiber electrode array for electrochemical detection of dopamine using fast scan cyclic voltammetry," *Analyst*, vol. 136, no. 9, pp. 1802–1805, Mar. 2011.
[18] Y. Xu, Z. Meng, Y. Meng, X. Li, and D. Xiao, "Lithium cobalt phosphate electrode for the simultaneous determination of ascorbic acid, dopamine, and serum uric acid by differential pulse voltammetry," *Microchimica Acta*, vol. 188, p. 190, May 2021.
[19] J. Yuen et al., "Cocaine-induced changes in tonic dopamine concentrations measured using multiple-cyclic square wave voltammetry in vivo," *Front. Pharmacol.*, vol. 12, Jul. 2021, Art. no. 705254.

[20] J. C. Chou, K. T. Lee, P. H. Yang, P. Y. Kuo, Y. H. Nien, and C. H. Lai, "Non-enzymatic ascorbic acid sensor simultaneous applied to potentiometric and amperometric measurement," *IEEE Trans. Nanotechnol.*, vol. 21, pp. 674–684, Nov. 2022.

[21] P. H. Yang, C. T. Chan, and Y. S. Chang, "A potentiometric uric acid biosensor integrated with temperature correction readout circuit on flexible PCB," *IEEE Sensors J.*, vol. 23, no. 9, pp. 9086–9092, May 2023.

[22] P. H. Yang, Y. S. Chang, and C. T. Chan, "Aluminum-doped zinc oxide enzymatic dopamine biosensor integrated with potentiometric readout circuit board," *IEEE Sensors J.*, vol. 23, no. 3, pp. 1809–1817, Feb. 2023.

[23] G. Jeevitha and D. Mangalaraj, "Ammonia sensing at ambient temperature using tungsten oxide (WO_3) nanoparticles," *Mater. Today, Proc.*, vol. 18, pp. 1602–1609, 2019.

[24] J. C. Chen, J. C. Chou, T. P. Sun, and S. K. Hsiung, "Portable urea biosensor based on the extended-gate field effect transistor," *Sensors Actuators B, Chem.*, vol. 91, pp. 180–186, Jun. 2003.

[25] J. Zou et al., "An ultra-sensitive electrochemical sensor based on 2D g-C_3N_4/CuO nanocomposites for dopamine detection," *Carbon*, vol. 130, pp. 652–663, Apr. 2018.

[26] Z. Yang, M. Li, H. Li, H. Li, C. Li, and B. Yang, "Polycrystalline boron-doped diamond-based electrochemical biosensor for simultaneous detection of dopamine and melatonin," *Analytica Chimica Acta*, vol. 1135, pp. 73–82, Oct. 2020.

[27] Z. Matouk, M. Islam, M. Gutiérrez, J. J. Pireaux, and A. Achour, "X-ray photoelectron spectroscopy (XPS) analysis of ultrafine au nanoparticles supported over reactively sputtered TiO_2 films," *Nanomaterials*, vol. 12, no. 20, pp. 1–12, Oct. 2022.

[28] S. Sun, X. Zhang, X. Song, S. Liang, L. Wang, and Z. Yang, "Bottom-up assembly of hierarchical Cu_2O nanospheres: Controllable synthesis, formation mechanism and enhanced photochemical activities," *CrystEngComm*, vol. 14, no. 10, pp. 3545–3553, Mar. 2012.

[29] B. Li, T. Liu, L. Hu, and Y. Wang, "A facile one-pot synthesis of Cu_2O/RGO nanocomposite for removal of organic pollutant," *J. Phys. Chem. Solids*, vol. 74, no. 4, pp. 635–640, Apr. 2013.

[30] D. W. Kim, K. Y. Rhee, and S. J. Park, "Synthesis of activated carbon nanotube/copper oxide composites and their electrochemical performance," *J. Alloys Compd.*, vol. 530, pp. 6–10, Jul. 2012.

[31] R. Sivakumar, R. Gopalakrishnan, M. Jayachandran, and C. Sanjeeviraja, "Investigation of X-ray photoelectron spectroscopic (XPS) Cyclic voltammetric analyses of WO_3 films and their electrochromic response in FTO/WO_3/electrolyte/FTO Cells," *Smart Mater. Structurest*, vol. 15, no. 3, pp. 877–888, May 2006.

[32] S. Bai et al., "Improvement of TiO_2 photocatalytic properties under visible light by WO_3/TiO_2 and MoO_3 /TiO_2 composites," *Appl. Surface Sci.*, vol. 338, pp. 61–68, May 2015.

[33] J. C. Chou et al., "Modifications to the scattering layer of a dye-sensitized solar cell photoanode with bifunctional WO_3 hollow spheres for increased electron transfer and scattering effect," *IEEE Trans. Electron Devices*, vol. 70, no. 5, pp. 2415–2423, May 2023.

[34] M. Durka, K. Durka, A. A.Woźniak, and W. Wróblewski, "Dopamine/2-phenylethylamine sensitivity of ion-selective electrodes based on bifunctional-symmetrical boron receptors," *Sensors*, vol. 19, p. 283, Jan. 2019.

[35] C. He, G. Li, Y. Wang, and W. Zhou, "A miniature potentiometric sensor for dopamine determination in vitro," *Meas. Sci. Technol.*, vol. 32, no. 6, Jun. 2021, Art. no. 065105.

[36] N. Dere, Z. Yolcu, and M. Yolcu, "A novel solid-state PVC-membrane potentiometric dopamine-selective sensor based on molecular imprinted polymer," *Acta Chimica Slovenica*, vol. 69, no. 1, pp. 108–115, Sep. 2022.

[37] H. K. Maleh, F. Karimi, M. Alizadeh, and A. L. Sanati, "Electrochemical sensors, a bright future in the fabrication of portable kits in analytical systems," *Chem. Rec.*, vol. 20, pp. 682–692, Jul. 2020.

[38] J. A. M. Pulgarín, A. A. Molina, E. J. García, and L. G. Gómez, "A sensitive resonance rayleigh scattering sensor for dopamine in urine using upconversion nanoparticles," *J. Raman Spectrosc.*, vol. 51, no. 3, pp. 406–413, Mar. 2020.

[39] J. C. Chou et al., "Novel potentiometric non-enzymatic ascorbic acid sensor based on molybdenum oxide film and copper nanoparticles," *IEEE Sensors J.*, vol. 22, no. 1, pp. 50–60, Jan. 2022.

[40] S. Wu et al., "Construction of cationic polyfluorinated azobenzene/reduced graphene oxide for simultaneous determination of dopamine, uric acid and ascorbic acid," *Talanta*, vol. 237, Jan. 2022, Art. no. 122986.

[41] Y. Yu, T. Nguyen, P. Tathireddy, S. Roundy, and D. J. Young, "A wireless battery-less and moisture-resistant packaged glucose sensing system employing hydrogel-based inductive sensing technique and low-power ASIC for long-term glucose monitoring," *Sensors Actuators A, Phys.*, vol. 341, Jul. 2022, Art. no. 113574.

[42] A. H. Diazcouder, R. R. Nava, R. Carbo, L. G. Sanchez-Lozada, and F. S. Munoz, "High fructose intake and adipogenesis," *Int. J. Mol. Sci.*, vol. 20, p. 2787, Jun. 2019.

[43] C. Bao, Q. Niu, Z. A. Chen, X. Cao, H. Wang, and W. Lu, "Ultrathin nickel-metal–organic framework nanobelt based electrochemical sensor for the determination of urea in human body fluids," *RSC Adv.*, vol. 9, pp. 29474–29481, Sep. 2019.

[44] C. Vanitha, A. Sanmugam, A. Yogananth, M. Rajasekar, P. G. Kuppusamy, and G. Devasagayam, "A facile synthesis of polyaniline-WO_3 hybrid nanocomposite for enhanced dopamine detection," *Mater. Lett.*, vol. 328, Dec. 2022, Art. no. 133149.

[45] T. C. Tsai, F. H. Huang, and J. J. J. Chen, "Selective detection of dopamine in urine with electrodes modified by gold nanodendrite and anionic self-assembled monolayer," *Sensors Actuators B, Chem.*, vol. 181, pp. 179–186, May 2013.

[46] Y. Zhao et al., "Highly stretchable and strain-insensitive fiber-based wearable electrochemical biosensor to monitor glucose in the sweat," *Anal. Chem.*, vol. 91, no. 10, pp. 6569–6576, Apr. 2019.

[47] R. Sha and S. Badhulika, "Facile green synthesis of reduced graphene oxide/tin oxide composite for highly selective and ultra-sensitive detection of ascorbic acid," *J. Alloys Compd.*, vol. 816, pp. 30–37, May 2018.

[48] N. Bhalla, P. Jolly, N. Formisano, and P. Estrela, "Introduction to biosensors," *Essays Biochem.*, vol. 60, pp. 1–68, Jun. 2016.

[49] L. Wang, M. Pagett, and W. Zhang, "Molecularly Imprinted Polymer (MIP) based electrochemical sensors and their recent advances in health applications," *Sensors Actuators Rep.*, vol. 5, Jun. 2023, Art. no. 100153.

[50] K. Ohshiro, Y. Sasaki, and T. Minami, "An extended-gate-type organic transistor-based enzymatic sensor for dopamine detection in human urine," *Talanta Open*, vol. 7, Aug. 2023, Art. no. 100190.

[51] P. Y. Kuo, M. T. Hsu, T. H. Wang, and C. H. Liao, "The sensing analysis of the potentiometric enzymatic RuO_2 biosensor based on FPCB for dopamine detection," *IEEE Trans. Electron Devices*, vol. 71, no. 1, pp. 790–796, Jan. 2024.

JUNG-CHUAN CHOU (Senior Member, IEEE) was born in Tainan, Taiwan, China, in July 1954. He received the B.S. degree in physics from Kaohisung Normal College, Kaohsiung, Taiwan, in 1976, the M.S. degree in applied physics from Chung Yuan Christian University, Chung-Li, Taiwan, in 1979, and the Ph.D. degree in electronics from National Chiao Tung University, Hsinchu, Taiwan, in 1988. From 1979 to 1991, he served as a Lecturer, an Associate Professor, and the Director with the Department of Electronic Engineering and Graduate School of Electronic Engineering, Chung Yuan Christian University. In 1991, he worked as an Associate Professor with the Department of Electronic Engineering, National Yunlin University of Science and Technology, Yunlin, Taiwan, where he has been a Professor since 2010, he was the Dean with the Office of Technology Cooperation from 1997 to 2002, he was the Chief Secretary from 2002 to 2009, he was the Director of Library from 2009 to 2010, and he was the Director of Office of Research and Development from 2010 to 2011. From 2013 to 2018, he was the Director of Administration, Testing Center for Technological and Vocational Education, where he has been a Deputy Director of Headquarters since 2018. From 2011 to 2017, he worked as a Distinguished Professor with the Department of Electronic Engineering, National Yunlin University of Science and Technology, where he was worked as a Lifetime Chair Professor in 2018. His research interests are in the areas of sensor material and device, biosensor and system, microelectronic engineering, optoelectronic engineering, solar cell, and solid state electronics.

WEI-SHUN CHEN was born in Yunlin County, Taiwan, in December 1999. He received the bachelor's degree from the Department of Aeronautical Engineering, National Formosa University. He is currently pursuing the master's degree with the Graduate School of Electronic Engineering, National Yunlin University of Science and Technology, Yunlin, Taiwan. His current research area is biosensor applications.

PO-HUI YANG (Member, IEEE) received the B.Eng. degree in marine electronics engineering from National Taiwan Ocean University in 1993, the M.S. degree in industrial education from National Taiwan Normal University in 1993, and the Ph.D. degree from the Institute of Electrical Engineering, National Chung Cheng University, in 2001. From 2001 to 2003, he was an Assistant Professor with the Department of Electronics, Southern Taiwan University of Science and Technology. From 2003 to 2004, he was a High-Performance Digital IC Design Engineer and the Circuit Design Section Manager with the SoC Technology Center, Industrial Technology Research Institute, Hsin-Chu, Taiwan. Afterward, he joined with the Department of Electronic Engineering, National Yunlin University of Science and Technology as an Assistant Professor and Associate Professor. His research interests include high-speed and low-power CMOS IC design, advanced IC packaging, and low-power biosensor IC design.

PO-YU KUO (Member, IEEE) was born in Taichung, Taiwan, in 1980. He received the M.S. and Ph.D. degrees in electrical engineering from the University of Texas at Dallas in 2006 and 2011, respectively. In 2013, he joined with the Department of Electronic Engineering, National Yunlin University of Science and Technology, Yunlin, Taiwan, where he is currently a Professor. His research interests include the analog circuits, power management circuits, and biosensor measurement.

CHIH-HSIEN LAI (Member, IEEE) was born in Taichung, Taiwan, in 1968. He received the B.S. and M.S. degrees in electrical engineering and the Ph.D. degree in photonics and optoelectronics from National Taiwan University, Taipei, Taiwan, in 1990, 1992, and 2010, respectively. He was worked with the Telecommunications Industry for a number of years, while also working extensively with the Department of Electronic Engineering, Hwa Hsia Institute of Technology, Taipei, Taiwan, from 2004 to 2012, as an Assistant Professor. In 2012, he joined with the Department of Electronic Engineering, National Yunlin University of Science and Technology, Yunlin, Taiwan, where he is currently a Professor. He served as a Chairman with the Department of Electronic Engineering from 2017 to 2020. His current research interests include the optical and terahertz guided-wave structures, nanophotonic devices, and optoelectronic devices.

YU-HSUN NIEN (Member, IEEE) received the Ph.D. degree from the Department of Material Sciences and Engineering, Drexel University, Philadelphia, PA, USA, in 2000. He is currently a Professor and the Director with the Center for Industrial Pollution Prevention Research, National Yunlin University of Science and Technology, Yunlin, Taiwan. His research interests include materials engineering and sustainable energy development.